



OPEN

## Poroelastic properties of rocks with a comparison of theoretical estimates and typical experimental results

A. P. S. Selvadurai<sup>1✉</sup> & A. P. Suvorov<sup>2</sup>

The paper develops theoretical estimates for the parameters that describe the classical theory of poroelasticity for a fluid-saturated porous medium, with a porous elastic skeleton that can exhibit imperfect grain contacts. The results for the poroelastic properties predicted from the modelling are compared with experimental results available in the literature.

The classical theory of poroelasticity proposed by M.A. Biot<sup>1</sup> is recognized<sup>2–10</sup> as a key development in the description of the continuum theory of fluid-saturated porous media. The scope of poroelasticity and related advances has found applications far beyond the originally envisaged topic of geological materials and soil mechanics. Developments in this area are too vast to cite in their entirety, and applications to diverse topics such as (1) mechanics of bone<sup>11</sup>, (2) hyperelastic soft tissues<sup>12–15</sup> (3) poroelastic media experiencing fracture, damage, failure and irreversible processes<sup>16–20</sup>, (4) geologic sequestration and ground subsidence<sup>21–27</sup>, (5) thermo-hydro-mechanics and geoenvironmental processes<sup>28–36</sup>, (6) contact and inclusion problems<sup>37–42</sup>, and (7) in the methodologies for the estimation of the material properties of Biot poroelasticity<sup>43–52</sup>, are briefly documented in the cited articles.

The estimation of the poroelasticity parameters can be a challenging exercise particularly when the rock has low permeability, when saturation of an initially dry pore space requires an inordinate amount of time<sup>49</sup>. Also, there are no assurances that the entire pore space becomes saturated during a saturation process and the presence of unsaturated regions can lead to erroneous estimates of the poroelastic parameters. Examples where alternative approaches can be adopted, for example, for the estimation of the permeability or the Biot coefficient of low permeability rocks are discussed in<sup>49–53</sup>. Therefore, any theoretical procedure that can be used to estimate poroelasticity properties of rocks will enhance the applicability of the theory.

### Analytical concepts

The classical theory of poroelasticity for an isotropic medium involves the skeletal deformability properties characterized by the skeletal or effective shear modulus ( $G^{eff}$ ), the skeletal or effective bulk modulus ( $K^{eff}$ ), the Biot coefficient  $\alpha$  and the permeability  $k$ . We develop analytical estimates for these isotropic poroelastic rocks and compare the estimates with experimental estimates of these properties for various rocks such as sandstones, limestones and granites-marbles that can be obtained from<sup>43,44</sup> and are presented in Tables 1 and 2, respectively. Missing properties in Table 2 are computed from available results using well known relationships applicable to isotropic elastic solids<sup>54,55</sup>. For example, the Biot modulus  $N$  in Table 2 is computed using the relationship

$$N = \frac{K^{eff} B}{\alpha(1 - \alpha B)}$$

where  $B$  is Skempton's pore pressure coefficient<sup>56</sup>. Analytical estimates of material properties of rocks can also be obtained using the microstructural models presented in<sup>57,58</sup> (see also<sup>59,60</sup>). In the microstructural models, the porous rock consists of non-porous solid grains, typically spherical in shape, and the space between the grains is identified as the pore space. The porosity of rock is denoted by  $\phi$ . The interface between the neighboring grains is assumed imperfect and characterized by a normal contact stiffness  $k_n$  and a tangential stiffness  $k_t$ , which can be developed by appeal to the classical studies by Mindlin<sup>61</sup> and Mindlin and Deresiewicz<sup>62</sup>. Schematic views

<sup>1</sup>Department of Civil Engineering and Applied Mechanics, McGill University, Montréal, QC H3A 0C3, Canada. <sup>2</sup>Department of Applied Mathematics, Moscow State University of Civil Engineering (MGSU), Moscow, Russia. ✉email: patrick.selvadurai@mcgill.ca

Rock	$G_{eff}$	$K_{eff}$	$\nu$	$K_u$	$\nu_u$	$K_m$	$\alpha$	$B$	$N$	$\phi$	$k$
Ruhr sandstone	13	13	0.12	30	0.31	36	0.65	0.88	41	0.02	1.97E-19
Tennessee marble	24	40	0.25	44	0.27	50	0.19	0.51	81	0.02	9.87E-22
Charcoal granite	19	35	0.27	41	0.30	45	0.27	0.55	84	0.02	9.87E-22
Berea sandstone	6.0	8.0	0.20	16	0.33	36	0.79	0.62	12	0.19	1.87E-16
Westerly granite	15	25	0.25	42	0.34	45	0.47	0.85	75	0.01	3.94E-21
Weber sandstone	12	13	0.15	25	0.29	36	0.64	0.73	28	0.06	9.87E-19
Ohio sandstone	6.8	8.4	0.18	13	0.28	31	0.74	0.50	9.0	0.19	5.53E-18
Pecos sandstone	5.9	6.7	0.16	14	0.31	39	0.83	0.61	10	0.20	7.89E-19
Boise sandstone	4.2	4.6	0.15	8.3	0.31	42	0.85	0.50	4.7	0.26	7.89E-16

**Table 1.** Poroelastic moduli for various rocks. Data is taken from<sup>44</sup>. [The elastic moduli are expressed in GPa. Permeability  $k$  is expressed in  $m^2$ ].

Rock	$G^{eff}$	$K^{eff}$	$K_m$	$\alpha$	$B$	$N$	$\phi$
Sandstone	6.3086	8.3	34.1	0.7566	0.67	14.9063	0.19
Sandstone	5.1506	6.7	26.3	0.7452	0.85	20.8484	0.19
Sandstone	5.6262	5.7	25.4	0.7756	0.76	13.6047	0.19
Sandstone	5.4703	6.7	30.1	0.7774	0.81	18.8520	0.19
Sandstone	5.1358	5.6	28.7	0.8049	0.68	10.4514	0.19
Limestone	11.0496	20.5	70.7	0.7100	0.49	21.6953	0.13
Limestone	13.0563	22.0	74.4	0.7043	0.42	18.6304	0.13

**Table 2.** Poroelastic moduli for various rocks. Data is taken from<sup>43</sup>. [Elastic moduli are expressed in GPa].

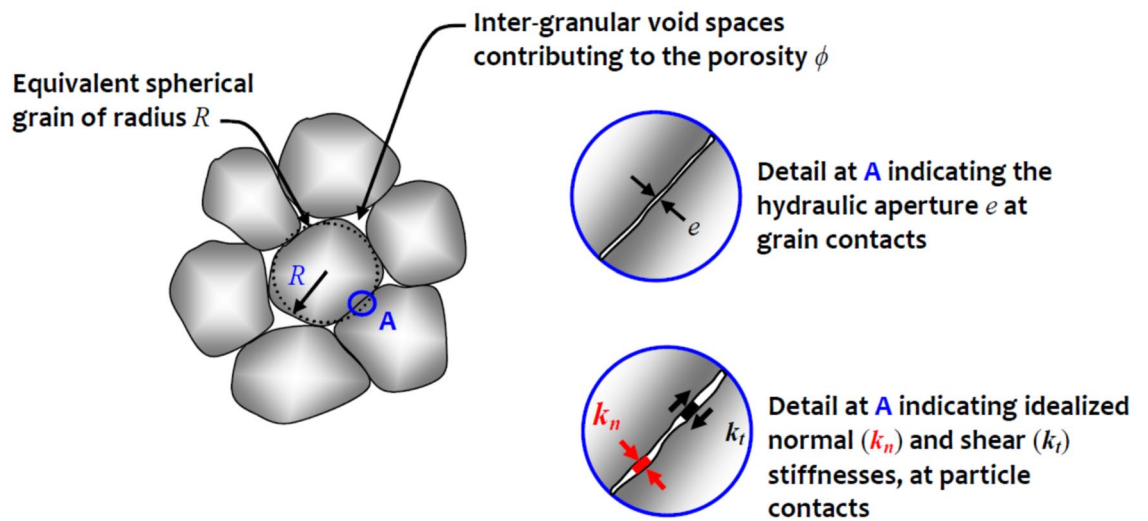


**Figure 1.** The idealized porous medium.

of the idealized concepts relating to the definitions of the granular assembly, porosity, contact stiffnesses and hydraulic aperture at grain contacts are shown in Fig. 1.

References to these studies and other relevant expositions on contact mechanics can be found in the studies<sup>63–68</sup>. Applications with special reference to geomaterials are given in<sup>69–71</sup>. The interfaces are considered to be very thin and are assumed to have no influence on the overall porosity  $\phi$ . Denoting the vector normal to the interface by  $\mathbf{n}$ , the traction vector acting on the interface is denoted by  $\mathbf{T}$ , the displacement jump at the interface is denoted by  $[\mathbf{u}]$  and the pore pressure is denoted by  $p$ . We can write the constitutive equations for the interface in the form

$$\begin{cases} \mathbf{T} \cdot \mathbf{n} = k_n[\mathbf{u} \cdot \mathbf{n}] - p & \text{for open or permeable interfaces} \\ \mathbf{T} \cdot \mathbf{n} = k_n[\mathbf{u} \cdot \mathbf{n}] & \text{for closed or impermeable interfaces} \\ \mathbf{T}_t = k_t[\mathbf{u}_t] \end{cases} \quad (1)$$

where  $\mathbf{T}_t = \mathbf{T} - (\mathbf{T} \cdot \mathbf{n})\mathbf{n}$  and  $\mathbf{u}_t = \mathbf{u} - (\mathbf{u} \cdot \mathbf{n})\mathbf{n}$ . Hence, if the interface is *permeable* or *open*, the fluid pressure contributes to the normal component of the traction vector, and if the interface is *impermeable* or *closed*, the fluid pressure has no influence at the interface. The *fraction of open interfaces* is denoted by  $r$ . Thus,  $r = 0$  if all the interfaces are closed, and  $r = 1$  if all the interfaces are open. Since the porosity measure utilizes only intra-granular spaces, (Fig. 1) the porosity is expected to have no influence on the interface stiffnesses  $k_n$  and  $k_t$ .

In addition, we can consider the stress  $\widehat{\mathbf{T}}$  acting on a grain  $G_i$  at the interface between the grains  $G_i$  and  $G_j$ . We can also relate this stress to the displacement jump  $[\mathbf{u}]$ . Let the coefficients of proportionality in these relations for the *normal* and *tangential* components of the stress vector  $\widehat{\mathbf{T}}$  be denoted by  $K_n$  and  $K_t$ , respectively. It is shown<sup>57</sup> that

$$K_n = \frac{k_n}{2} \quad ; \quad K_t = \frac{k_t}{2} \quad (2)$$

Estimates of the elastic properties are obtained from a self-consistent method that is applicable to particulate aggregates developed in<sup>72-74</sup> and summarized in<sup>75</sup>. The following normalized quantities are introduced

$$K = \frac{K^{eff}}{K_n R}; \quad M = \frac{G^{eff}}{K_n R}; \quad \rho = \frac{K_t}{K_n} = \frac{k_t}{k_n} \quad (3)$$

where  $R$  is the radius of the grain. Experimental values for the grain sizes of most rocks is provided by granulometric data. In what follows, we make the assumption that the grains are rigid. In this case, the self-consistent estimate of the shear modulus can be obtained by solving the following cubic equation:

$$16M^3 + 4\{2 + 3\phi + 2\rho(3\phi - 1)\}M^2 + \{3(3\phi - 1) + 2\rho(12\phi - 5)\}M + 3\rho(2\phi - 1) = 0 \quad (4)$$

Once the normalized shear modulus  $M$  is known, the self-consistent estimate of the bulk modulus can be obtained from

$$K = \frac{4(1 - \phi)M}{3(2M + \phi)} \quad (5)$$

From the above relationship, we have

$$M = \frac{2(1 - \phi)}{3} \left( \frac{M}{K} \right) - \frac{\phi}{2} = \frac{2(1 - \phi)}{3} \left( \frac{G^{eff}}{K^{eff}} \right) - \frac{\phi}{2} \quad (6)$$

Therefore, if the effective shear modulus  $G^{eff}$  and the effective bulk modulus  $K^{eff}$  are known from experiments, one can determine the constant  $M$  from (6) and consequently estimate the ratio  $\rho = k_t/k_n$  using (4): i.e.

$$\rho = \frac{16M^3 + 4(2 + 3\phi)M^2 + 3(3\phi - 1)M}{8(1 - 3\phi)M^2 + 2(5 - 12\phi)M + 3(1 - 2\phi)} \quad (7)$$

It should be noted<sup>76,77</sup> that self-consistent schemes are not without flaws and should be judiciously applied when extreme limiting cases are being considered.

### Numerical results for deformability behaviour

Figure 2 shows estimates of interface stiffness ratio  $\rho = k_t/k_n$  plotted against the porosity  $\phi$ . The estimates are obtained from (7), based on the values of bulk and shear moduli listed in Table 1<sup>44</sup> and Table 2<sup>43</sup>. It can be observed that the ratio  $\rho$  ranges between 0.3 and 0.6 for sandstones and is approximately equal to 0.1 for limestones and granites-marbles.

It is also instructive to plot the ratio  $\rho$  as a function of the parameter  $(G^{eff}/K^{eff}) = (M/K)$ . Figure 3 shows the ratio  $\rho$  plotted against  $(M/K)$ . It turns out that  $\rho$  is approximately a linear function of the parameter  $(M/K)$ .

The interfacial stiffness  $K_n R$  can be obtained from the definition of  $M$  (3), i.e.,

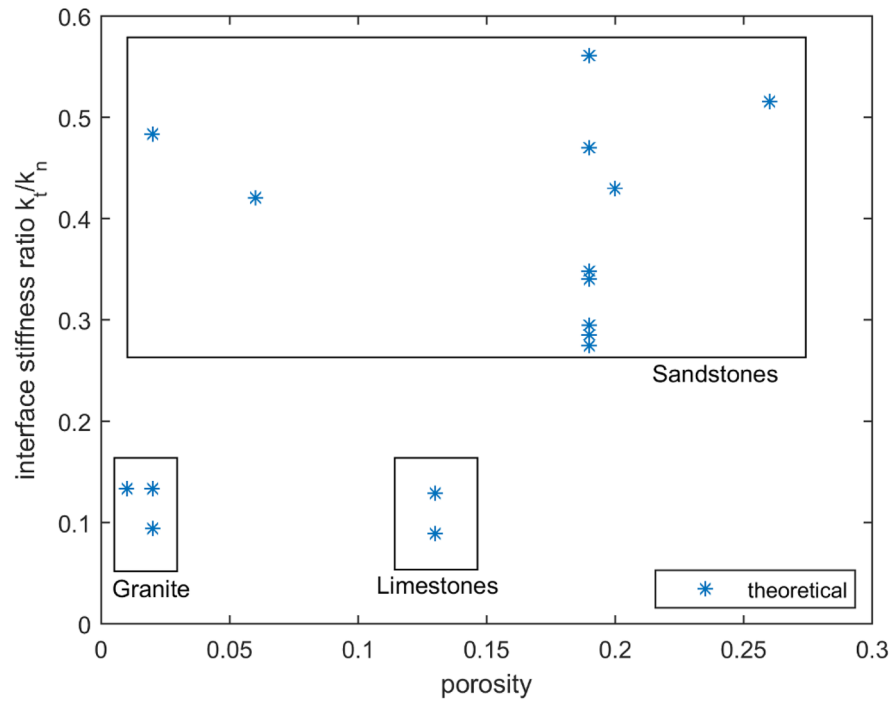
$$K_n R = \frac{k_n R}{2} = \frac{G^{eff}}{M} \quad (8)$$

Using (6), we also obtain the ratio of the interfacial stiffness  $K_n R$  to the effective bulk modulus as follows:

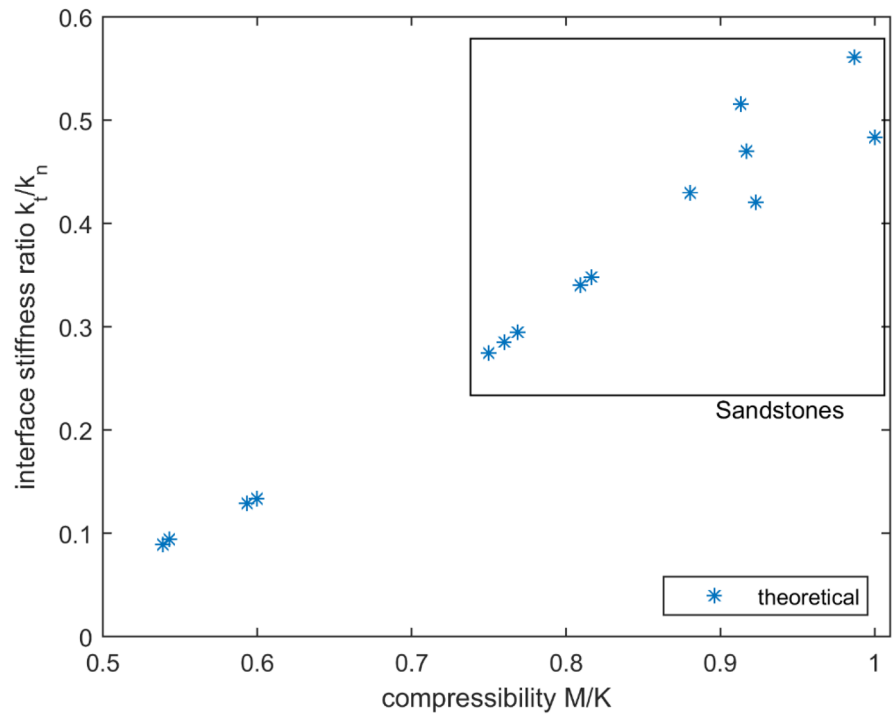
$$\frac{K_n R}{K^{eff}} = \frac{G^{eff}}{K^{eff} M} = \frac{G^{eff}}{\left( \frac{2(1-\phi)}{3} G^{eff} - \frac{\phi}{2} K^{eff} \right)} \quad (9)$$

Figure 4 shows the variation in the normalized interfacial stiffness  $(K_n R/K^{eff})$  with porosity  $\phi$ . It can be seen that this dependency can be conveniently approximated by a linear relationship.

When the grains are rigid, the estimate for the Biot coefficient  $\alpha$  can be obtained in the form



**Figure 2.** Ratio of interface stiffnesses  $\rho$  versus porosity.



**Figure 3.** Ratio of interface stiffnesses  $\rho$  versus compressibility parameter  $(G^{eff}/K^{eff}) = (M/K)$ .

$$\alpha = 1 - \frac{3K}{2}(1 - r) \tag{10}$$

where  $r$  is the fraction of open or permeable interfaces,  $0 \leq r \leq 1$ . Using the expression for the constant  $M$  given by (6), we can represent the Biot coefficient as

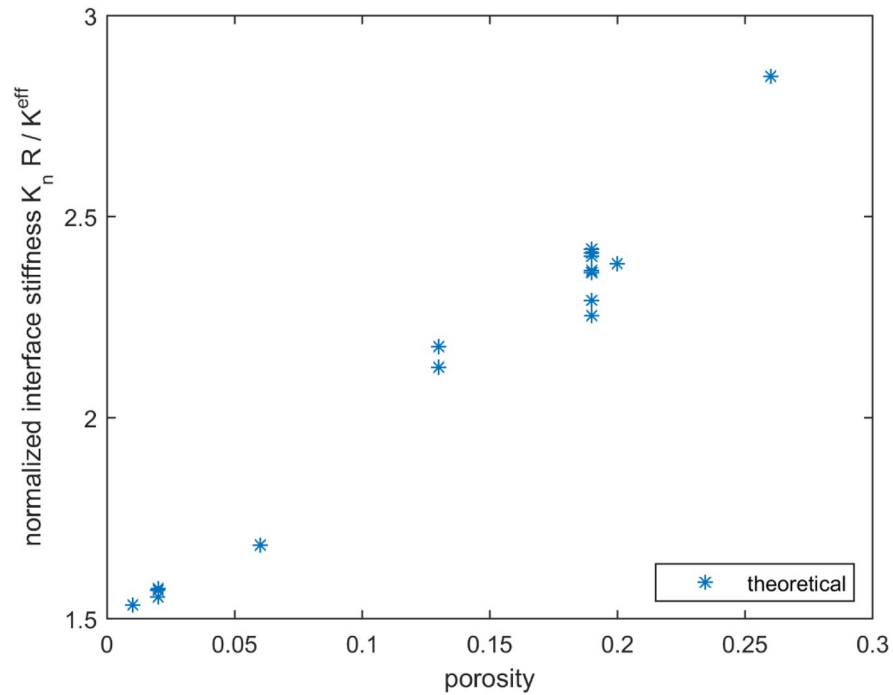


**Figure 4.** Normalized interfacial stiffness ( $K_n R / K^{eff}$ ) versus porosity.

$$\alpha = 1 - \left\{ 1 - \phi \left( 1 + \frac{3 K^{eff}}{4 G^{eff}} \right) \right\} (1 - r) \tag{11}$$

If the Biot coefficient is known from experimental data<sup>10,43,44,50,51,78,79</sup>, the fraction of open interfaces  $r$  can be estimated from (11) as

$$r = \left\{ \frac{\alpha - \phi \left( 1 + \frac{3 K^{eff}}{4 M^{eff}} \right)}{1 - \phi \left( 1 + \frac{3 K^{eff}}{4 M^{eff}} \right)} \right\} \tag{12}$$

Figure 5 shows estimates for the parameter  $r$  for rocks given in Tables 1 and 2. The parameter  $r$  is plotted as a function of the porosity  $\phi$  and the value of  $r$  is obtained from (12) by matching the Biot coefficient  $\alpha$  with the experimental values, indicated in Tables 1 and 2. The grains are modelled as nearly spherical shapes and the pore space is also modelled as a nearly spherical shape. The results can be influenced by the shape of the pores and this was addressed in a previous study<sup>53</sup>.

In Fig. 6 we indicate the dependency of the Biot coefficient  $\alpha$  on the porosity  $\phi$ . This figure demonstrates that by properly choosing the microstructural parameters  $M$  (or  $K$ ),  $\rho$  and  $r$  it is possible to exactly match the elastic constants  $K^{eff}$ ,  $G^{eff}$  and  $\alpha$  with the experimental data. It can be observed from Fig. 6 that, on average, for sandstones and limestones the Biot coefficient is equal to 0.75 and for the marbles-granite group the Biot coefficient can be lower and in the range 0.2 to 0.5. This observation is consistent with results obtained recently for the Lac du Bonnet granite recovered from the Canadian Shield<sup>79</sup>.

The self-consistent estimate of Biot modulus  $N$  can be obtained from the relationship<sup>57</sup>

$$\frac{1}{N} = \frac{3\alpha}{2} (1 - r) \left( \frac{1 - \frac{\phi}{\left\{ 1 - \frac{3K}{2} \right\}}}{K_n R} \right) = \frac{3\alpha}{2} (1 - r) \left( \frac{1 - \phi \left( \frac{1-r}{\alpha-r} \right)}{K_n R} \right) \tag{13}$$

When the estimates for the Biot modulus  $N$  obtained from the relationship (13) are compared with the experimental values of  $N$  there is a large discrepancy. To eliminate this discrepancy, the compressibility of the fluid phase must be taken into account, which gives another expression for the Biot modulus

$$\frac{1}{N} = \frac{\phi}{K_f} + \frac{3\alpha}{2} (1 - r) \left( \frac{1 - \phi \left( \frac{1-r}{\alpha-r} \right)}{K_n R} \right) \tag{14}$$

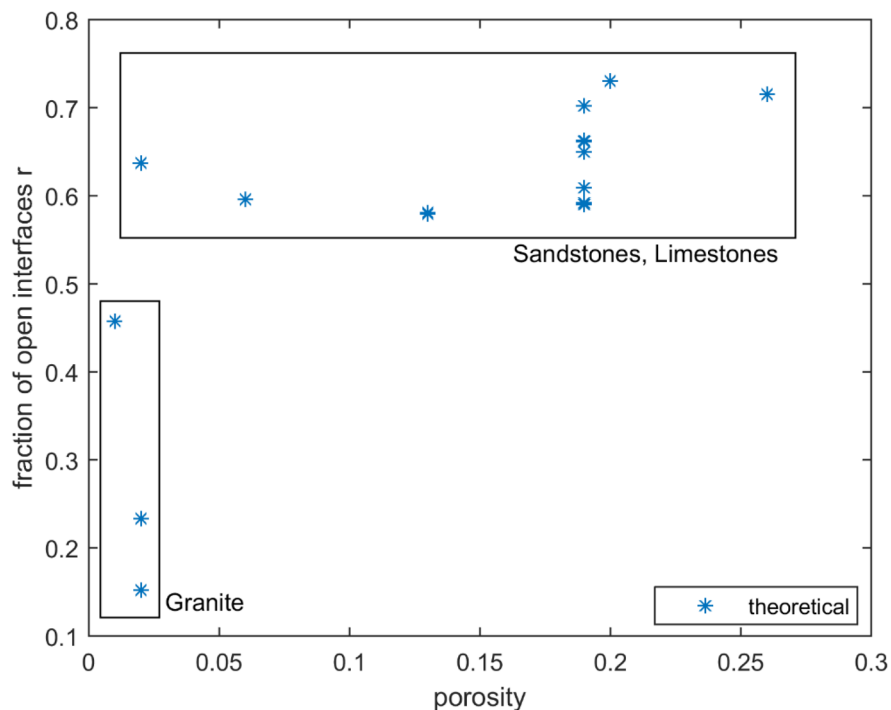


**Figure 5.** Fraction of open interfaces  $r$  versus porosity. [The limestones data points are easy to identify by the porosity value of 0.13. Keeping two types of rocks (sandstones and limestones) in one group seems possible in this case because they have similar values for fraction of open interfaces].

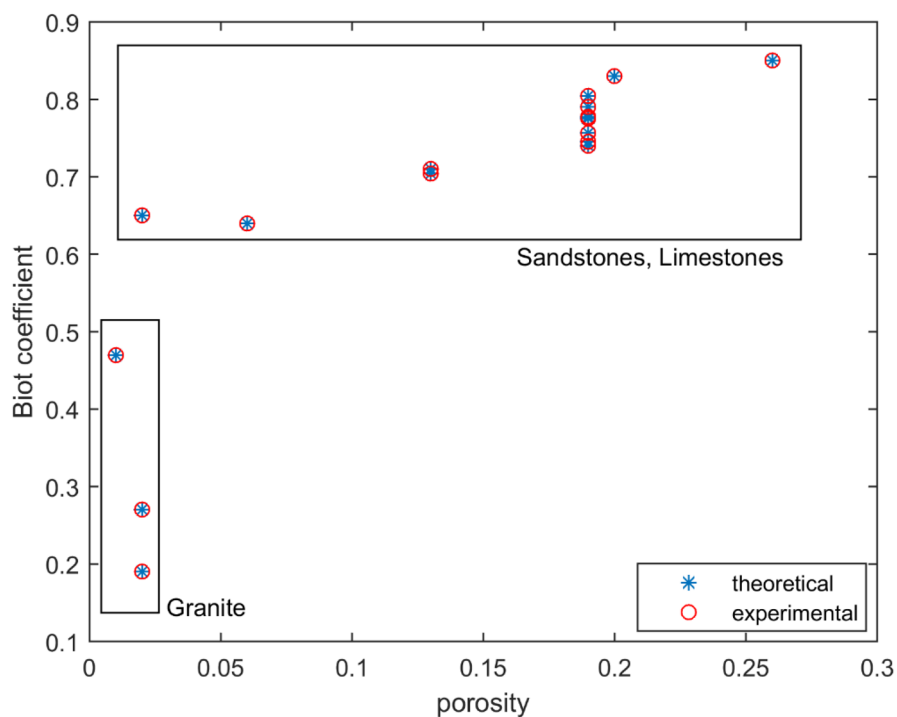


**Figure 6.** Biot coefficient  $\alpha$  versus porosity.

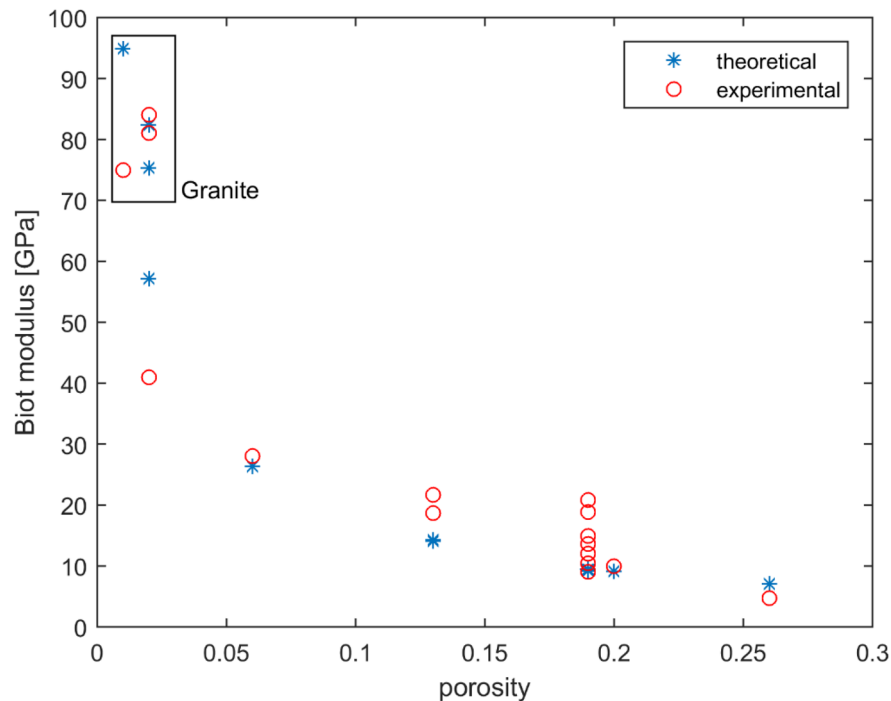


**Figure 7.** Biot modulus  $N$  versus porosity.

where  $K_f$  is the bulk modulus of the fluid. The interface stiffness  $K_n R$  was estimated first from Eq. (9). This value is then substituted into (13) or (14) to estimate the Biot modulus  $N$ . Thus, a knowledge of the grain size radius is not required.

Figure 7 shows experimental values of the Biot modulus  $N$  and the corresponding theoretical estimates for  $N$  obtained from (14). Theoretical values are obtained by setting the bulk modulus of the fluid  $K_f = 2$  GPa, which is typically applicable to water. An acceptable agreement between the theoretical and experimental values is obtained by choosing this constant value of  $K_f$ .

### Estimates for permeability

The self-consistent estimate of permeability  $k$  is obtained as

$$k = \frac{2}{1 - 3\phi} \frac{r\eta}{R} \quad (15)$$

where  $\eta$  is the interface permeability, which can be related to the aperture of the contact through the usual parallel plate model<sup>55,80–83</sup>, i.e.

$$\eta = \frac{e^3}{24} \quad (16)$$

Here  $e$  is the spacing between two neighboring grains (joint opening) and  $R$  is the grain radius. By substituting (16) into (15) we obtain

$$k = \frac{r}{12(1 - 3\phi)} \frac{e^3}{R} \quad (17)$$

The result (17) contains the additional factors that can influence permeability, including the grain size, bulk porosity and a measure of the fraction of open interfaces. If these parameters can be accurately estimated, the result gives an added perspective for estimating permeability. Since the equation for permeability (17) is used as an equality constraint in the optimization problem and the solution to the optimization problem exists, then the proper choice of grain radius and joint opening allows us to match the permeability obtained from theoretical estimates (17) with the experimental data.

It should be noted that the definition of the hydraulic aperture does not account for any fine particles that can be present in sandstone and carbonate rocks. As has been suggested<sup>84</sup>, an average value for the joint opening can be set as  $e = 0.5 \mu\text{m}$  and for the radius  $R = 50 \mu\text{m}$ . It should be noted that these assigned values are typical of tight sandstones and should not be construed as an “average value”. They fulfil the function of normalizing values. However, by using these particular values it is not possible to match experimental values of permeability,

Rock	$R_n$	$e_n$
Ruhr sandstone	2.269007	0.146912
Tennessee marble	5.960993	0.055916
Charcoal granite	6.638004	0.050212
Berea sandstone	1.000000	0.836472
Westerly granite	5.510982	0.060483
Weber sandstone	1.544066	0.215891
Ohio sandstone	1.176403	0.283350
Pecos sandstone	2.055110	0.162203
Boise sandstone	1.000000	1.052523

**Table 3.** Deviations of radius of the grain  $R$  and joint opening  $e$  from their nominal values of  $50 \mu\text{m}$ , and  $0.50 \mu\text{m}$ , respectively.

presented in Table 1, with the theoretical estimate (17). Thus, we can introduce the following quantities, which represent deviations from established values

$$R_n = \frac{R}{50 \mu\text{m}} \quad ; \quad e_n = \frac{e}{0.5 \mu\text{m}} \quad (18)$$

When the results (18) are substituted into (17), we obtain

$$k = \frac{r}{12(1-3\phi)} \frac{e_n^3(0.5)^3}{50R_n} \times 10^{-12} \quad (19)$$

We can rewrite (19) as an equality constraint in terms of variables  $R_n$  and  $e_n^3$ : i.e.

$$\frac{600k(1-3\phi)}{r(0.5)^3} 10^{12} R_n - e_n^3 = 0 \quad (20)$$

Here  $k$  is the value of permeability measured experimentally. As the objective function to be minimized, we can take the sum of deviations of variables  $R_n$  and  $e_n$  from unity i.e.,

$$\min : S = R_n(\text{if } R_n \geq 1) + \frac{1}{R_n}(\text{if } R_n < 1) + e_n(\text{if } e_n \geq 1) + \frac{1}{e_n}(\text{if } e_n < 1) \quad (21)$$

We note that  $R_n$  and  $e_n^3$  must be positive, which constitutes inequality constraints.

Solution to this non-linear optimization problem for the rocks presented in Table 1 is shown in Table 3. The solution was obtained with the help of MATLAB function `fmincon`. It may be observed that  $R_n$  and  $e_n$  are close to unity only for Berea sandstone and Boise sandstone. For other sandstones, the radius  $R$  can be twice  $50 \mu\text{m}$  and the spacing between neighboring grains can be 5–7 times smaller than the normative value of  $0.5 \mu\text{m}$ . The largest deviations are observed for the granite-marble group. Here, the grain radius  $R$  is about 5 to 6 times larger than the normative value of  $50 \mu\text{m}$ , and  $e$  is, on average, 20 times smaller than  $0.5 \mu\text{m}$ .

### Concluding remarks

The estimation of the poroelasticity properties of rocks can proceed along two avenues; the first involves their direct evaluation from experimental data and the second approach is to utilize the theories developed for multiphase composites to arrive at estimates for the poroelasticity parameters. Both approaches have their advantages and disadvantages. The purely experimental approach is void of consideration of the micro-mechanical input to the poroelastic parameters but provides the data set that can be used in the engineering calculation of poroelastic responses. The approaches based on multiphase theories have to rely on idealized theoretical assumptions that lead to parameter estimates but adds a new dimension by introducing the properties of the fabric that compose the poroelastic material. The prudent option is to rely on both approaches and to take advantage of the merits of each approach to provide the validations that will enable the assignment of poroelastic parameter estimates. The results of the paper provide correlations between (1) porosity of a poroelastic solid and the grain-grain contact stiffnesses at the particulate level, (2) the interface stiffness ratio and effective shear to bulk modulus ratio, (3) open interface fraction and porosity, (4) the variation of the Biot coefficient and Biot modulus on porosity and (5) the dependency of permeability on microstructural properties. The research utilizes the material data available in the literature and provides the summary related to (1) to (4) in terms of the basic rock types relevant to sedimentary (sandstones, limestones) and igneous (granite, basalt) rocks. The data presented enables the preliminary identification of poroelastic parameters, which can be complemented by a rigorous program of laboratory tests. In the absence of experimental data for poroelastic properties of a particular rock, the findings of the research can be treated as a data set for preliminary geosciences calculations that requires recourse to the theory of linear poroelasticity. Since the original experimental data does not contain ranges or error estimates, the study can provide only firm values of the parameters. The measurement of the properties of saturated rocks with low permeability is generally a challenging task in the laboratory since it is difficult to ensure that the sample is fully saturated during testing. Such theoretical approaches can have practical applications in geotechnical

engineering and rock mechanics. Finally, the paper presents a canonical methodology for including additional parameters in the development of concepts for examining poroelastic parameters. In efforts of this nature, the microstructural parameters are introduced within the framework of a plausible concept. The progress of the modelling will require novel experimental methodologies, in the area of geomechanics and material science for accurately estimating the parameters arising from the developments.

Received: 31 January 2022; Accepted: 15 June 2022

Published online: 29 June 2022

## References

1. Biot, M. A. General theory of three-dimensional consolidation. *J. Appl. Phys.* **12**, 155–164 (1941).
2. Paria, G. Flow of fluid through porous deformable media. *Appl. Mech. Rev.* **16**, 901–907 (1963).
3. Schiffman, R. L. A bibliography of consolidation. In *Fundamentals of Transport Phenomena in Porous Media* (eds Bear, J. & Corapcioglu, M. Y.) 617–669 (Martinus Nijhoff Publ, 1984).
4. Selvadurai, A. P. S. (ed.) *Mechanics of Poroelastic Media* (Kluwer Academic Publishers, 1996).
5. Coussy, O. *Mechanics of Porous Media* (Wiley, 1995).
6. Wang, H. F. *Theory of Linear Poroelasticity with Applications to Geomechanics and Hydrogeology* (Princeton University Press, 2000).
7. Dormieux, L., Kondo, D. & Ulm, F. J. *Microporomechanics* (Wiley, 2006).
8. Selvadurai, A. P. S. The analytical methods in geomechanics. *Appl. Mech. Rev.* **60**, 87–106 (2007).
9. Verruijt, A. *Theory and Problems in Poroelasticity* (Delft University of Technology, 2015).
10. Cheng, A. H. D. *Poroelasticity Vol. 27* (Springer International Publ, 2016).
11. Cowin, S. C. (ed.) *Bone Mechanics Handbook* 2nd edn. (CRC Press, 2001).
12. Selvadurai, A. P. S. & Suvorov, A. P. Coupled hydro-mechanical effects in a poro-hyperelastic material. *J. Mech. Phys. Solids* **91**, 311–333 (2016).
13. Suvorov, A. P. & Selvadurai, A. P. S. On poro-hyperelastic shear. *J. Mech. Phys. Solids* **96**, 445–459 (2016).
14. Selvadurai, A. P. S. & Suvorov, A. P. On the inflation of poro-hyperelastic annuli. *J. Mech. Phys. Solids* **107**, 229–252 (2017).
15. Selvadurai, A. P. S. & Suvorov, A. P. On the development of instabilities in an annulus and a shell composed of a poro-hyperelastic materials. *Proc. Roy. Soc. Ser. A* **474**, 20180239 (2018).
16. Atkinson, C. & Craster, R. V. Plane strain fracture in poroelastic media. *Proc. Roy. Soc. Ser. A* **434**, 605–663 (1991).
17. Selvadurai, A. P. S. & Mahyari, A. T. Computational modelling of the indentation of a cracked poroelastic halfspace. *Int. J. Fract.* **86**, 59–74 (1997).
18. Selvadurai, A. P. S. & Shirazi, A. Mandel-Cryer effects in fluid inclusions in damage-susceptible poroelastic media. *Comput. Geotech.* **31**, 285–300 (2004).
19. Selvadurai, A. P. S. & Samea, P. Mechanics of a pressurized penny-shaped crack in a poroelastic halfspace. *Int. J. Eng. Sci.* **163**, 103472 (2021).
20. Selvadurai, A. P. S. Irreversibility of soil skeletal deformations: The pedagogical limitations of Terzaghi's celebrated model for soil consolidation. *Comput. Geotech.* **135**, 104137 (2021).
21. Geertsma, J. Land subsidence above compacting oil and gas reservoirs. *J. Petrol. Technol.* **25**, 734–744 (1973).
22. Segall, P. Induced stresses due to fluid extraction from axisymmetric reservoirs. *Pure Appl. Geophys.* **139**, 535–560 (1992).
23. Segall, P. & Fitzgerald, S. D. A note on induced stress changes in hydrocarbon and geothermal reservoirs. *Tectonophysics* **289**, 117–128 (1998).
24. Rutqvist, J. & Tsang, C. F. A study of caprock hydromechanical changes associated with CO<sub>2</sub> injection into a brine aquifer. *Environ. Geol.* **42**, 296–305 (2002).
25. Rutqvist, J., Birkholzer, J., Cappa, F. & Tsang, C.-F. Estimating maximum sustainable injection pressure during geologic sequestration of CO<sub>2</sub> using coupled fluid flow and geomechanical fault slip analysis. *Energy Convers. Manag.* **48**, 1798–1807 (2007).
26. Selvadurai, A. P. S. & Kim, J. Poromechanical behaviour of a surficial geological barrier during fluid injection into an underlying poroelastic storage formation. *Proc. Roy. Soc. Ser. A* **472**, 20150418 (2016).
27. Selvadurai, A. P. S. & Kim, J. Ground subsidence due to uniform fluid extraction over a circular region within an aquifer. *Adv. Water Resour.* **78**, 50–50 (2015).
28. Selvadurai, A. P. S. & Nguyen, T. S. Computational modelling of isothermal consolidation of fractured porous media. *Comp. Geotech.* **17**, 39–73 (1995).
29. Nguyen, T. S. & Selvadurai, A. P. S. Coupled thermal-mechanical-hydrological behaviour of sparsely fractured rock: Implications for nuclear fuel waste disposal. *Int. J. Rock Mech. Min. Sci. Geomech. Abstr.* **32**, 465–479 (1995).
30. Selvadurai, A. P. S., Hu, J. & Konuk, I. Computational modelling of frost heave induced soil-pipeline interaction II. Modelling of experiments at the Caen test facility. *Cold Regions Sci. Tech* **29**, 229–257 (1999).
31. Selvadurai, A. P. S. & Suvorov, A. P. Boundary heating of poro-elastic and poro-elasto-plastic spheres. *Proc. Roy. Soc. Ser. A* **468**, 2779–2806 (2012).
32. Selvadurai, A. P. S. & Suvorov, A. P. Thermo-poromechanics of a fluid-filled cavity in a fluid-saturated geomaterial. *Proc. Roy. Soc. Ser. A* **470**, 20130634 (2014).
33. Najari, M. & Selvadurai, A. P. S. Thermo-hydro-mechanical response of granite to temperature changes. *Environ. Earth Sci.* **72**, 189–198 (2014).
34. Selvadurai, A. P. S., Suvorov, A. P. & Selvadurai, P. A. Thermo-hydro-mechanical processes in fractured rock formations during glacial advance. *Geosci. Model Dev.* **8**, 2168–2185 (2015).
35. Selvadurai, A. P. S. & Suvorov, A. P. *Thermo-Poroelasticity and Geomechanics* (Cambridge University Press, 2017).
36. Selvadurai, A. P. S. & Najari, M. The thermo-hydro-mechanical behaviour of the argillaceous Cobourgh Limestone. *J. Geophys. Res. Solid Earth*. <https://doi.org/10.1002/2016JB013744> (2017).
37. Chiarella, C. & Booker, J. R. The time-settlement behaviour of a rigid die resting on a deep clay layer. *Quart. J. Mech. Appl. Math.* **28**, 317–328 (1975).
38. Selvadurai, A. P. S. & Yue, Z. Q. On the indentation of a poroelastic layer. *Int. J. Numer. Anal. Methods Geomech.* **18**, 161–175 (1994).
39. Yue, Z. Q. & Selvadurai, A. P. S. On the mechanics of a rigid disc inclusion embedded in a fluid saturated poroelastic medium. *Int. J. Eng. Sci.* **33**, 1633–1662 (1995).
40. Selvadurai, A. P. S. & Shi, L. Biot's problem for a Biot Material. *Int. J. Eng. Sci.* **97**, 133–147 (2015).
41. Kim, J. & Selvadurai, A. P. S. A note on the consolidation settlement of a rigid circular foundation on a poroelastic halfspace. *Int. J. Numer. Anal. Methods Geomech.* **40**, 2003–2016 (2016).
42. Selvadurai, A. P. S. & Samea, P. On the indentation of a poroelastic halfspace. *Int. J. Eng. Sci.* **149**, 103246 (2020).
43. Hart, D. J. & Wang, H. F. Laboratory measurements of a complete set of poroelastic moduli for Berea sandstone and Indiana limestone. *J. Geophys. Res.* **100**, 17741–17751 (1995).

44. Zimmermann, R. W. Micromechanics of poroelastic rocks. In *Heterogeneous Media: Micromechanics Modeling Methods and Simulations* (eds Markov, K. & Preziosi, L.) 411–469 (Birkhauser, 2000).
45. Mavko, G., Mukerji, T. & Dvorkin, J. *The Rock Physics Handbook: Tools for Seismic Analysis of Porous Media* (Cambridge University Press, 2009).
46. Saxena, N. Exact results for generalized Biot-Gassmann equations for rocks that change in pore shape and grain geometry. *Geophys. J. Int.* **203**, 1575–1586 (2015).
47. Selvadurai, A. P. S. & Najari, M. Isothermal permeability of the argillaceous Cobourg limestone. *Oil Gas Sci. Technol. Spec. Issue Permeabil. Geomater.* **71**, 53–69 (2016).
48. Selvadurai, A. P. S. & Najari, M. Laboratory-scale hydraulic pulse testing: Influence of air fraction in cavity on the estimation of permeability. *Geotechnique* **65**, 126–134 (2015).
49. Selvadurai, A. P. S. The Biot coefficient for a low permeability heterogeneous limestone. *Contin. Mech. Thermodyn.* **31**, 939–953 (2019).
50. Selvadurai, A. P. S., Selvadurai, P. A. & Nejati, M. A multi-phasic approach for estimating the Biot coefficient for Grimsel granite. *Solid Earth*. **10**, 2001–2014 (2019).
51. Suvorov, A. P. & Selvadurai, A. P. S. The Biot coefficient for an elasto-plastic material. *Int. J. Eng. Sci.* **145**, 103166 (2019).
52. Selvadurai, A. P. S. A multi-phasic perspective of the intact permeability of the heterogeneous argillaceous Cobourg Limestone. *Sci. Rep.* **9**, 17388 (2019).
53. Selvadurai, A. P. S. & Suvorov, A. P. The influence of the pore shape on the bulk modulus and the Biot coefficient of fluid-saturated porous rocks. *Sci. Rep.* **10**, 18959 (2020).
54. Davis, R. O. & Selvadurai, A. P. S. *Elasticity and Geomechanics* (Cambridge University Press, 1996).
55. Selvadurai, A. P. S. *Partial Differential Equations in Mechanics, Vol. 2. The Biharmonic Equation, Poisson's Equation* (Springer, 2000).
56. Skempton, A. W. The pore pressure coefficients A and B. *Geotechnique* **4**, 143–147 (1954).
57. He, Z., Dormieux, L., Lemarchand, E. & Kondo, D. A poroelastic model for the effective behaviour of granular materials with interface effect. *Mech. Res. Comm.* **43**, 41–45 (2012).
58. Jeannin, L. & Dormieux, L. Poroelastic behaviour of granular media with poroelastic interfaces. *Mech. Res. Commun.* **83**, 27–33 (2017).
59. Gurevich, B. & Schoenberg, M. Interface conditions for Biot equations of poroelasticity. *J. Acoust. Soc. Am.* **105**, 2585–2589 (1999).
60. Selvadurai, A. P. S. Interface porosity and the Dirichlet/Neumann pore fluid pressure boundary conditions in poroelasticity. *Transp. Porous Media* **71**, 161–172 (2008).
61. Mindlin, R. D. Compliance of elastic bodies in contact. *J. Appl. Mech.* **16**, 259–268 (1949).
62. Mindlin, R. D. & Deresiewicz, H. Elastic spheres in contact under varying oblique forces. *J. Appl. Mech.* **20**, 327–344 (1953).
63. Lur'e, A. I. *Three-Dimensional Problems of the Theory of Elasticity* (Wiley Interscience, 1964).
64. Selvadurai, A. P. S. *Elastic Analysis of Soil-Foundation Interaction* (Elsevier Scientific Publishing, 1979).
65. Gladwell, G. M. L. *Contact Problems in the Classical Theory of Elasticity* (Sijthoff and Noordhoff, 1980).
66. Johnson, K. L. *Contact Mechanics* (Cambridge University Press, 1985).
67. Aleynikov, S. M. *Spatial Contact Problems in Geomechanics: Boundary Element Method* (Springer, 2011).
68. Barber, J. R. *Contact Mechanics* (Springer, 2018).
69. Selvadurai, A. P. S. & Boulon, M. J. *Mechanics of Geomaterial Interfaces, Vol. 42. Studies in Applied Mechanics* (Elsevier Science Publ., Amsterdam, 1995).
70. Selvadurai, A. P. S., Selvadurai, P. A. & Suvorov, A. P. Contact mechanics of a dilatant region located at a compressed elastic interface. *Int. J. Eng. Sci.* **133**, 144–168 (2018).
71. Selvadurai, A. P. S. In-plane loading of a bonded rigid disc inclusion embedded at a pre-compressed elastic interface: The role of non-linear interface responses. *Mech. Syst. Signal Process.* **144**, 106871 (2020).
72. Hershey, A. V. The elasticity of an isotropic aggregate of anisotropic cubic crystals. *J. Appl. Mech.* **21**, 236–240 (1954).
73. Hill, R. Self-consistent mechanics of composite materials. *J. Mech. Phys. Solids* **13**, 213–222 (1965).
74. Kröner, E. Self-consistent scheme and graded disorder in polycrystal elasticity. *J. Phys. F Met. Phys.* **8**, 2261–2267 (1978).
75. Kanaun, S. K. & Levin, V. M. *Self-Consistent Methods for Composites. Volume 1-Static Problems, Solid Mechanics and Its Applications* Vol. 148 (Springer, 2008).
76. Budiansky, B. On the elastic moduli of some heterogeneous materials. *J. Mech. Phys. Solids* **13**, 223 (1965).
77. Christensen, R. M. *Mechanics of Composite Materials* (Wiley, 1979).
78. Rice, J. R. & Cleary, M. P. Some basic stress diffusion solutions for fluid saturated elastic porous media with compressible constituents. *Rev. Geophys.* **14**, 227–241 (1976).
79. Selvadurai, A. P. S. On the poroelastic Biot coefficient for a granitic rock. *Geosciences* **11**, 219 (2021).
80. Bear, J. *Dynamics of Fluids in Porous Media* (Dover Publications, 1972).
81. Philips, O. M. *Flow and Reactions in Permeable Rocks* (Cambridge University Press, 1991).
82. Nguyen, T. S. & Selvadurai, A. P. S. A model for coupled mechanical and hydraulic behaviour of a rock joint. *Int. J. Numer. Anal. Methods Geomech.* **22**, 29–48 (1998).
83. Ichikawa, Y. & Selvadurai, A. P. S. *Transport Phenomena in Porous Media: Aspects of Micro/Macro Behaviour* (Springer, 2012).
84. Dormieux, L., Jeannin, L. & Gland, N. Homogenized models of stress-sensitive reservoir rocks. *Int. J. Eng. Sci.* **49**, 381–396 (2011).

## Acknowledgements

The work described in the paper was supported by a Discovery Research Grant awarded by the Natural Sciences and Engineering Research Council of Canada. The research support provided by the Moscow State University of Civil Engineering is also duly acknowledged. The authors are grateful to two reviewers for their highly constructive comments.

## Author contributions

The concepts related to the paper were developed by A.P.S.S. and A.P.S. The numerical evaluations were performed by A.P.S. and verified by A.P.S.S. The paper was written and revised by A.P.S.S. and A.P.S. All authors agreed to the format and presentation of the final manuscript.

## Competing interests

The authors declare no competing interests.

## Additional information

**Correspondence** and requests for materials should be addressed to A.P.S.S.

**Reprints and permissions information** is available at [www.nature.com/reprints](http://www.nature.com/reprints).

**Publisher's note** Springer Nature remains neutral with regard to jurisdictional claims in published maps and institutional affiliations.



**Open Access** This article is licensed under a Creative Commons Attribution 4.0 International License, which permits use, sharing, adaptation, distribution and reproduction in any medium or format, as long as you give appropriate credit to the original author(s) and the source, provide a link to the Creative Commons licence, and indicate if changes were made. The images or other third party material in this article are included in the article's Creative Commons licence, unless indicated otherwise in a credit line to the material. If material is not included in the article's Creative Commons licence and your intended use is not permitted by statutory regulation or exceeds the permitted use, you will need to obtain permission directly from the copyright holder. To view a copy of this licence, visit <http://creativecommons.org/licenses/by/4.0/>.

© The Author(s) 2022